Citation: Salman Khayoon Aldriasawi, Nihayat Hussein Ameen, Kareem Idan Fadheel, et al. An experimental artificial neural network model: investigating and predicting effects of quenching process on residual stresses of AISI 1035 steel alloy. *Journal of Harbin Institute of Technology (New Series)*. DOI:10.11916/j.issn.1005-9113.2023090

An Experimental Artificial Neural Network Model: Investigating and Predicting Effects of Quenching Process on Residual Stresses of AISI 1035 Steel Alloy

Salman Khayoon Aldriasawi[1*], *Nihayat Hussein Ameen*[2], *Kareem Idan Fadheel*[1], *Ashham Muhammed Anead*[1], *Hakeem Emad Mhabes*[3] *and Barhm Mohamad*[4]

(*1.Mechanical Engineering Department, Kut Technical Institute, Middle Technical University, Baghdad 10074, Iraq*;
2.College of Agriculture, University of Kirkuk, Kirkuk 36001, Iraq; *3.Computer Science Department, Kut Technical Institute, Middle Technical University, Baghdad 10074, Iraq*;
4.Department of Petroleum Technology, Koya Technical Institute, Erbil Polytechnic University, Erbil 44001, Iraq)

Abstract: The present study establishes a new estimation model using an artificial neural network (ANN) to predict the mechanical properties of the AISI 1035 alloy. The experiments were designed based on the L16 orthogonal array of the Taguchi method. A proposed numerical model for predicting the correlation of mechanical properties was supplemented with experimental data. The quenching process was conducted using a cooling medium called "nanofluids". Nanoparticles were dissolved in a liquid phase at various concentrations (0.5, 1, 2.5, and 5 % vf) to prepare the nanofluids. Experimental investigations were done to assess the impact of temperature, base fluid, volume fraction, and soaking time on the mechanical properties. The outcomes showed that all conditions led to a noticeable improvement in the alloy's hardness which reached 100%, the grain size was refined about 80%, and unwanted residual stresses were removed from 50 to 150 MPa. Adding 5% of CuO nanoparticles to oil led to the best grain size refinement, while adding 2.5% of Al_2O_3 nanoparticles to engine oil resulted in the greatest compressive residual stress. The experimental variables were used as the input data for the established numerical ANN model, and the mechanical properties were the output. Upwards of 99% of the training network's correlations seemed to be positive. The estimated result, nevertheless, matched the experimental dataset exactly. Thus, the ANN model is an effective tool for reflecting the effects of quenching conditions on the mechanical properties of AISI 1035.

Keywords: Quenching, nanofluids, residual stresses, steel alloy, artificial neural network, MANOVA
CLC number: TG156.3 **Document code**: A **Article ID**: 1005-9113(2023)00-0000-16

0 Introduction

Quenching is a vital process used to improve carbon steel's microstructure, hardness, and other mechanical properties. The AISI 1035 steel alloy has found widespread application in the manufacture of mechanical structures for forged parts. It is utilized for couplings, gears, links, and shafts. The phase changes and the microstructures of the materials are impacted by the sudden cooling. The improvement of the mechanical characteristics produced by the quenching process depends on a number of variables, including the quenching temperature, the chemical composition of the steel alloy, the thermophysics of the cooling medium, and the rate of cooling[1-3]. The influence of carbon nanotubes (CNTs) on the microstructure, surface roughness, and hardness of AISI 1010 is investigated in this study via quenching. Three different levels of cooling medium are used, namely distilled water and surfactant with CNTs, distilled water with CNTs, and distilled water. The

Received 2023-08-30.
* Corresponding author. Salman Khayoon Aldriasawi, Ph.D, Lecturer, E-mail: Salman.khayoon@mtu.edu.iq

outcome showed that surface roughness, hardness, and microstructures vary with the cooling medium and CNT concentrations, this demonstrated that quenching by CNTs imposes higher roughness than quenching by water. However, specimens quenched by CNTs with a surfactant have harder surfaces[4]. Previous literature has proposed the quenching of medium carbon steel for the design of optimal heat treatment conditions using the Taguchi technique. Whereby the coolant fluids were engine oil, de-ionized water, and salt solution as base fluid and with dispersed nanoparticles of TiO_2, αAL, and CuO. The experimental temperatures were 400, and 550 ℃. The soaking times were 60, 45, and 30 min, respectively. The experimental outcomes showed that the nanoparticle type TiO_2, tempering time 30 min, tempering temperature (400 ℃), and base fluid engine oil and salt solution positively affect yield strength and ultimate strength. Meanwhile, nanoparticle type CuO, tempering time of 60 min, tempering temperature of 550 ℃, and base fluid deionized water have a significant effect on elongation in medium carbon steel[5]. The lubricating viscosity can be increased by incorporating copper oxide nanoparticles into 10w40 engine oil. A multilayer perception algorithm-based ANN prediction model was proposed[6]. In order to maximize the hardness, laboratory - grade carbon nanoparticles were utilized with water as the base fluid for AISI 1045. The concentrations of carbon content varied from 0.1% to 0.5%. The outcome showed that a maximum hardness of about 885.34 HV might be achieved with a concentration value of 0.2%. At the same time, the microstructure of AISI 1045 after quenching mainly consisted of martensite[7]. The carbon steel was heated to 1000 ℃ and quenched in different mediums to determine a suitable quenching medium for carbon steel. The results presented that increasing the ferrite phase structures leads to a decreased hardness of steel. Therefore, after quenching using water and nanofluids, a martensite phase formed, which caused an increase in the hardness of steel by about 728 HV[8]. There are two ways to make nanofluid: the one-step method and the two - step method. In the one - step procedure, nanoparticles are created while being spread evenly throughout the base liquid. While in the later, the nanoparticles are created and subsequently mixed with the basic liquid[9]. For medium carbon steel, hybrid heat treatment was utilized to enhance the mechanical qualities of CK 35. Samples of carbon steel were subjected to a standard heat treatment at 830 ℃ and quenched in an oil medium. In order to enhance the mechanical properties of the steel, these samples were once again treated by generating impulse signals on the surface[10]. Tempering temperature values have an impact on the microstructures and characteristics as well [11]. It has been demonstrated that different quenching media affect the mechanical behavior of carbon steel AISI1030 differently. Specimens were heated in an electrical furnace for 1 h to 950 ℃. The specimens were cooled using polyvinyl chloride, water, and oil. After an hour tempered at 200 ℃, the specimens were quenched in air. The outcome showed that quenching by water increased the hardness constant, yield stress, and ultimate stress while lowering Young's modulus E. Additionally, the pearlite and ferrite phases of the crystalline structure, as well as the grain size (refining), were improved by water quenching followed by tempering[12]. An extensive study addressing all facets of quenching using vegetable oil was discussed[13]. An analysis of the distortion, phase change, hardness, and microstructure of AISI 4410 as a result of the quenching process was conducted numerically using the Finite Element Method. The validity of the simulation was confirmed by experimental verification of the simulated results. The outcomes demonstrated strong convergence between the simulation and experimental results[14]. The volume fraction of pearlite, bainite, and ferrite in the steel rotor shaft 30CrMoNiV5-11 was predicted using ANN[15]. The impact of heat treatment on the mechanical characteristics of A357 alloy was estimated using an ANN model with a back - propagation technique. According to the results, a back-propagation model might be adopted in the prediction approach[16]. ANN was used to predict the anisotropic mechanical properties of Inconel 718 alloy at a temperature between room temperature to 600 ℃, and the result of the model confirmed the result of the f-test and t-test[17]. The mechanical properties of titanium alloy have been widely exploited in engineering applications. Therefore, a model was proposed to minimize the cost and time for predicting mechanical properties using ANN and a back-propagation algorithm. The percentage error was less than 10%; this might be used to predict and estimate the mechanical properties of titanium alloy[18]. An ANN

model was utilized to analyze sensitivity and parametric based on experiment's result of shot peening process[19-21]. Deep Cryogenic process was utilized to improve residual stresses and hardness of too steel. The result observations were increasing micro, and macro hardness about 27 HV, and 0.5 HRC respectively. While the amount of residual stress was descend about 35%[22]. An experimental and statistical investigation on steel alloy was done. The effect of machining parameter was optimized and analyzed by Taguchi method and ANOVA[23].

In this study, experimental work was conducted to figure out the effect of different quenching mediums using nanofluids such as water/TiO_2, CuO/Oil, Al_2O_3/Oil engine, water/hybrid nanoparticles on the mechanical properties of AISI 1035 steel alloy. Taguchi array is utilized to design the experiments set and analyses the effect of quenching conditions. Sixteen experiments were conducted to optimize the effect on the residual stresses, hardness, and microstructures. The results of experiments have been analyzed by MANOVA in the MINITAB19 to figure out the largest effect of quenching parameters on mechanical properties. Moreover, an ANN is used to develop original numerical model to estimate how mechanical characteristics will behave during the quenching process. The proposed numerical model for predicting the correlation of mechanical properties is supplemented by experimental data. Both theoretical and experimental investigations can benefit the usage of the experimental data and the suggested ANN model. The ANN performance is evaluated by different statistics criteria such as R^2, and RMSE.

1 Materials and Experimental

1.1 Materials

Medium carbon steel AISI1035 was purchased from Alhadad for Materials Co., Ltd, Baghdad, Iraq. The chemical composition and mechanical properties of the specimens are listed in Tables 1 and 2. The chemical composition analysis was carried out at Al-Nasser Company for Engineering Inspections.

Table 1 Chemical composition of AISI 1035

Content	Fe	Si	C	Mn	S	P
Standard Percent (%)[24]	Bal.	0.07- 0.6	0.32-0.38	0.6-0.9	< 0.05	<0.04
Measured (%)	Bal.	0.21	0.35	0.64	0.026	0.11

Table 2 Mechanical properties of AISI 1035[24]

Yield strength (MPa)	Shear yield strength (MPa)	Ultimate tensile stress (MPa)	Ultimate shear stress (MPa)	Hardness (H.V)	Elongation(%)
550	339.8	620	406.8	188	13

1.2 Nanofluid Preparation

Four different categories of nanofluids were used in this investigation. Nanoparticles were acquired from US Research Nanomaterial, Inc. Details about the materials, oxides, and base fluids are included in Table 3. Metallic oxides increase their thermal conductivity and viscosity as their specific size decreases[25]. The nanoparticule size has an impact on the thermophysics of nanofluids. Al_2O_3, TiO_2, and CuO were consequently mechanically milled for a period of 60 min. The nanoparticles were gradually added to the base fluid, which was either distilled water or engine oil, and mixed for 180 min using a magnetic stirrer to produce a homogenous liquid. Water distillation was used to produce the distilled water. To prevent the deposition of nanoparticles, the samples were submerged directly in the nanofluid. The L16 orthogonal array was chosen in this study to optimize the samples´ hardness, microstructures, and residual stresses. Nanofluid type, nanoparticular concentrations, and soaking period were all taken into account.

Table 3 Properties of nano-particular and base fluid

Metal oxides and base fluids	Size(nm)	Purity(%)	Color
TiO_2	15	99.5	White
Al_2O_3	80	99.0	White
CuO	40	99.0	Black
Hybrid nanocomposite (CuO/ TiO_2)			Grey
Distilled water			
Engine oil			

2 Experimental Design

The Taguchi method is an efficient technique that is frequently used in engineering analysis to help reduce the number of experiments and save time. An orthogonal array is regarded by this method ´s experiment design as being reliable, simple to analyze, and easy to comprehend. The number of elements in the study will determine how many experiments need to be conducted, so it is important to carefully control the significant factors. The signal to noise function (S/N) can be used to measure how far the sleeved parameters are from their ideal values using the loss function[26]. S/ N small is the best utilized for grain size and residual stresses, while S/N large is better used for hardness response. Equations 1 and 2 are used to calculate the responses of S/N[27]. In this study, the design of experiments used the L16 orthogonal array. Four factors were chosen in order to examine their effects on the mechanical properties, namely concentration ratio, nanofluid type, quenching temperature, and soaking time. Only one factor had two levels, while the other three factors had four levels. Tables 4 and 5 include an explanation of the factors and their levels, as well as the number of required runs. A mixed design (1^2 3^4) of the L16 orthogonal array included sixteen experiments.

$$\frac{S}{N} = -10\log\frac{1}{n}\sum_{i=1}^{n} y_i^2 \tag{1}$$

$$\frac{S}{N} = -10\log\frac{1}{n}\sum_{i=1}^{n} 1/y_i^2 \tag{2}$$

where n is number of runs; y is experimental output.

Table 4 Quenching factors and their levels

Level	Concentration C(%)	Nanofluid type L	Temperature T(℃)	Soaking time S(min)
Level 1	0.5	Water/ TiO_2	850	30
Level 2	1.0	Oil / CuO	900	60
Level 3	2.5	Oil engine/ Al_2O_3	950	
Level 4	5.0	Water/ hybrid nano	1000	

Table 5 Orthogonal array of Taguchi L_{16}

No.	Concentration(%)	Nanofluids	Temperature(℃)	Time(min)
1	C_1	L_1	T_1	S_1
2	C_1	L_2	T_2	S_1
3	C_1	L_3	T_3	S_2
4	C_1	L_4	T_4	S_2
5	C_2	L_1	T_2	S_2
6	C_2	L_2	T_1	S_2
7	C_2	L_3	T_4	S_1
8	C_2	L_4	T_3	S_1
9	C_3	L_1	T_3	S_1
10	C_3	L_2	T_4	S_1
11	C_3	L_3	T_1	S_2
12	C_3	L_4	T_2	S_2
13	C_4	L_1	T_4	S_2
14	C_4	L_2	T_3	S_2
15	C_4	L_3	T_2	S_1
16	C_4	L_4	T_1	S_1

Hybrid nanoparticles were used to obtain further thermal properties of single nanoparticles[28]. Nanofluid comprising nanoparticular TiO_2 + CuO based water was used to quench one category of the experimental specimens. An Olympus SZ61, an optical microscope, was used to observe the microstructures and calculate the grain size. In order to conduct the microstructure test and to determine the morphology of the surface by scanning electronic microscopy (SEM), the research specimens were

prepared in three steps: mounting, grinding, and polishing. The surfaces of the specimens were wet ground on SiC sheets with grit sizes 180, 320, 600, 800, and 1100. On a rotary pre-grinder polisher, the specimens were polished using Al_2O_3 alumina powder (0.6, 0.3, 0.1 m). In the preliminary stage, the surface was polished to remove contamination using an ultrasonic machine. Finally, to reveal the morphology and grain structures of the specimens, a 2% Nital solution was used to etch the polished surfaces. An optical microscopy device with a 100 X magnification factor was used to gather the results. Fig. 1 illustrates the AISI1035 microstructure. A Zwick & Co.'s Z323 hardness tester was used to determine the surface hardness. Standard Test Method ASTM E92 is utilized for hardness test. Under a weight of 0.9 kg, the hardness of the quenched samples was evaluated. Three different hardness measurements were made, and the average value was calculated. The XRD method was used to measure the residual stresses near the surface of the alloy using an XRD 6000 (ORION, model RKS 1500 F-V -SP).

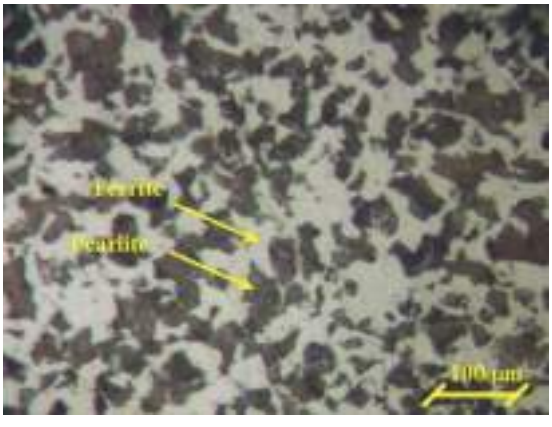

Fig.1 Microstructure of steel alloy[1]

3 Artificial Neural Network (ANN) Model

ANNs can be reformed for huge, complex, and nonlinear databases. Moreover, it can be used for prediction and optimization requirements[29-31]. ANN is consisting of input layer, hidden layer, and output layer[32]. Traditionally, ANN is consisting of one input layer, one or more hidden layer based on the ANN performance may modified, output layer is result of ANN model[33-34]. Activation function is used based on the maximum R^2 value, and minimum Root Mean Square RMS value[35-36]. ANN architecture is feeding with r, p, d and s parameters as input parameter, weight w, and bias b, linear combiner factor, transfer function f, and output a.

3.1 ANN Modeling and Implementation

To determine the best outcomes from the experimental attempts, four input subsets of parameters (time, temperature, nanofluid type, and concentration ratio) were used, which was expensive and time-consuming. Since previous researchers have utilized the artificial numerical approach, it might be possible to determine the ideal input parameters to achieve optimal outputs. In this context, Fig. 2 provides a summary of the ANN model employed in this investigation. As one of the tests for each network system, it contains one output, one hidden layer, and four input parameters. The four neurons in the input layer represent the concentration values, the type of nanofluid, the temperature, and the soaking duration, respectively. Ten neurons make up the buried layer. The output layer, however, only contains one neuron because it is accurate in estimating mechanical features.

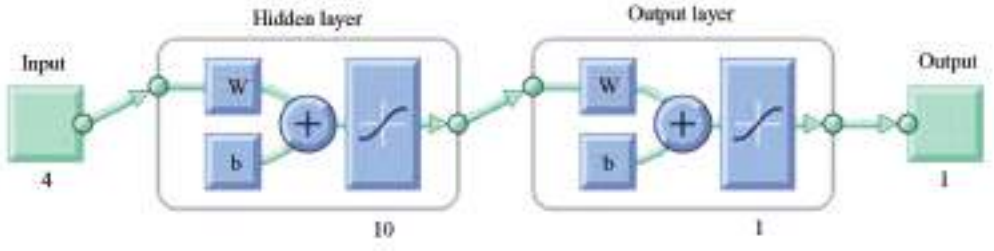

Fig. 2 Proposed ANN model framework

The Training function Levenberg-Marquardt backpropagation) trainFcn = 'trainlm'(with learning rate 0.1, training time 1000 s, learning epoch 10000 epoch, stopping criterion based on MSE criteria goal equal to zero, and transfer function sigmoid, these parameters are adopted to establish ANN model.

For improved training results[37], the feed-forward background was taken into consideration when developing the network scheme. Only 16 experimental data could be applied to the network for the training goal due to the extremely constrained experimental conditions. The results of the observations of the output neurons from the ANN algorithm included residual stress, grain size, and hardness. The ANN estimation was tested using the same 16 experimental data, and the method's errors were determined.

4 Results

4.1 Quenching Result

The results of the proposed quenching method exhibited a significant enhancement in hardness, a refinement of the grain size, and the removal of unwanted residual stresses, the results are listed in Table 6.

Table 6 Results of the experimental work on a trained dataset of the control parameters and their values

No.	Concentration Vf (%)	Nanofluids	Temperature C(℃)	Time(min)	Mechanical properties		
					H. V (kg/mm^2)	RSes. (MPa)	Grain (μm)
1	0.5	Water + TiO_2	850	30	476.380	53	20.15
2	1.0	Water + TiO_2	900	30	404.460	−173	19.62
3	2.5	Water + TiO_2	950	60	550.520	−67	18.02
4	5.0	Water + TiO_2	1000	60	416.275	110	19.60
5	0.5	Oil+CuO	900	60	589.140	−35	20.11
6	1.0	Oil+CuO	850	60	491.500	−113	16.31
7	2.5	Oil+CuO	1000	30	454.970	−86	17.28
8	5.0	Oil+CuO	950	30	448.160	−239	16.52
9	0.5	Oil engine + Al_2O_3	950	30	476.380	72	17.16
10	1.0	Oil engine + Al_2O_3	1000	30	599.430	81	15.27
11	2.5	Oil engine + Al_2O_3	850	60	515.580	−57	14.85
12	5.0	Oil engine + Al_2O_3	900	60	532.620	−96	15.96
13	0.5	Water + CuO	1000	60	523.990	42	15.42
14	1.0	Water+ hybrid nanoparticular (75% CuO+25% TiO_2)	950	60	679.660	53	15.24
15	2.5	Water+ hybrid nanoparticular (50% CuO+50% TiO_2)	900	30	454.970	68	16.35
16	5.0	Water+ hybrid nanoparticular (25% CuO+75% TiO_2)	850	30	550.525	85	15.02

The outcome also indicated the enhancement of the hardness, grain size, and residual stresses of the AISI 1035 steel alloy during analysis of ANOVA. The heat treatment process is descending to refine grain size and becomes harder. Also, it is lead to remove the tension stresses[38-41]. Phase transformation, especially in the steel, from the austenite to metastable martensite phase takes place. This action is highly recommended because it enhances hardness of steel[2]. The obtained result is in agreement with previous studies on hardness improvement. Thus, the best conditions for quenching by a nanofluid of water/TiO_2 is by adding 0.2% of TiO_2 nanoparticles and using a holding time of one hour. The grain size was measured based on the result of optical microstructures. The results showed refinements of grain size for most specimens. Fig. 3(a) shows the morphology of the surfaces of the steel AISI 1035 under heat treatment (quenching) in a nanofluid of water/TiO_2. The percentage of elements (C) appears to be higher than those of the other elements, as seen in the EDS for the light region. Because of the portion (C), the residual stress was reduced, and the grain size was large. The high proportion of (C) due to the reaction of the

media (water/TiO_2) during the quenching operation means that the nanofluid is less perfect for producing reasonable hardness and refined grain size. Fig. 3(b) shows the effect of heat treatment in the media (Oil/CuO). The percentage of (C) was still high, but the rate of (Mn) increased, and (Fe) decreased, which caused a high reduction in residual stress and a low grain size; hence, this medium was better than the other. It can be seen in Fig. 3(c) that the percentage of element (Fe) was high; it is suggested that the residual stress was so high that the effect of the quenching media was not enough to spread the heat regularly. The (Fe) in Fig. 3(d) was extremely high. The main change involved the elements (Mn), (Fe), and (C). Numerous studies have been conducted to identify these phase transitions and establish a link between them and the mechanical properties of steel alloys[42].

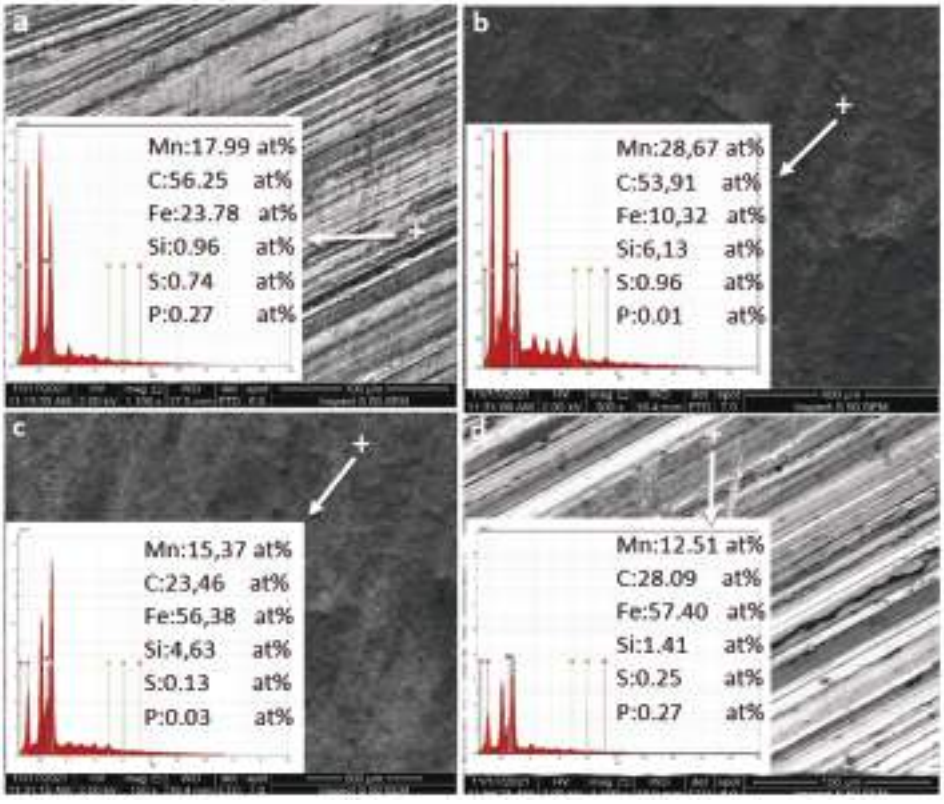

Fig. 3 SEM of treated specimens by nanofluid

The process of quenching results in the production of martensite. The ideal hardness value was introduced when carbon was present during the quenching of oil with alumina oxide. The formation of martensite and the carbon content led to an increase in hardness. Increased carbon content makes an alloy harder, but the martensite proportion must be properly managed. Additionally, manganese has a weaker ability to increase the steel's hardness. The properties of steel alloy are influenced by residual stresses. Exchanging of heat transfer among quenching parameters and steel surface is considering a key source to relief residual stresses[2]. As a result, eliminating undesired residual stresses from the manufacturing process is one of the main goals of the heat treatment procedure[2,43-44]. Residual tensile stresses are eliminated, and compressive residual stresses are generated by quenching in copper oxide oil. The slight increase in manganese allowed for the greatest compressive stresses. The mechanical properties of a steel alloy may be influenced by the grain size microstructure. As can be seen from the findings of the experimental study, the refinement of the grain size increases the resistance and hardness of steel. Fig. 4 shows a plot of how the concentration ratio, nanofluid medium, temperature, and soaking duration affect the hardness, grain size, and residual stresses. The outcome showed that for entire cases, agreed with literature studies, the concentration ratio significantly influenced the hardness, residual

stresses, and grain size. The type and temperature of the nanofluids had less of an impact than the concentration ratio. On the other hand, the amount of time spent soaking only had an impact on the outcome of hardness. A statistical analysis MANOVA is implanted by MINITAB19 software to study the significance of the studied factors on hardness, grain size and residual stresses. Three criteria Wilks ´, Lawley-Hotelling, and Pillai´s are used. The main significant factor is nanofluid type at $\alpha = 0.05$ with p value of 0.029 based on Wilks´ criteria, 0.01 based on Lawley-Hotelling criteria.

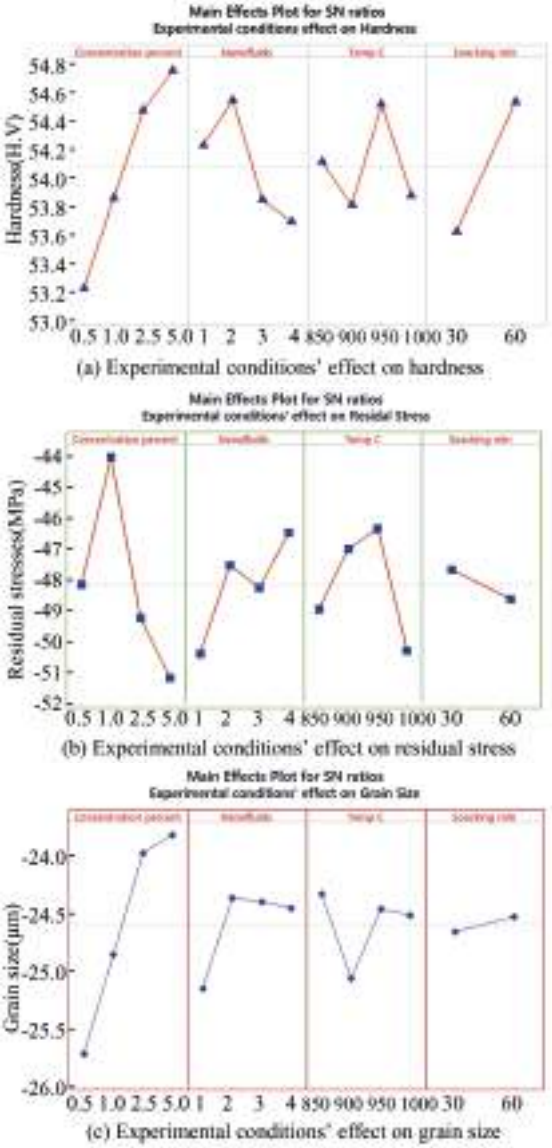

(a) Experimental conditions' effect on hardness

(b) Experimental conditions' effect on residual stress

(c) Experimental conditions' effect on grain size

Fig. 4 Effects of experiments conditions on hardness, residual stress and grain size

4.2 Prediction Results of ANN Model

In order to make an estimation of hardness, Residual stresses, and Grain size, the ANN training has been realized using 16 different samples, as shown in Table 5. Figs.5(a)-(c) display how each ANN network is implemented. These charts demonstrate how closely the output of the model matches the actual goal values. The best outcome, where outputs = targets, is shown by the dashed line in each figure. A solid line illustrates the difference between the target and output linear regressions.

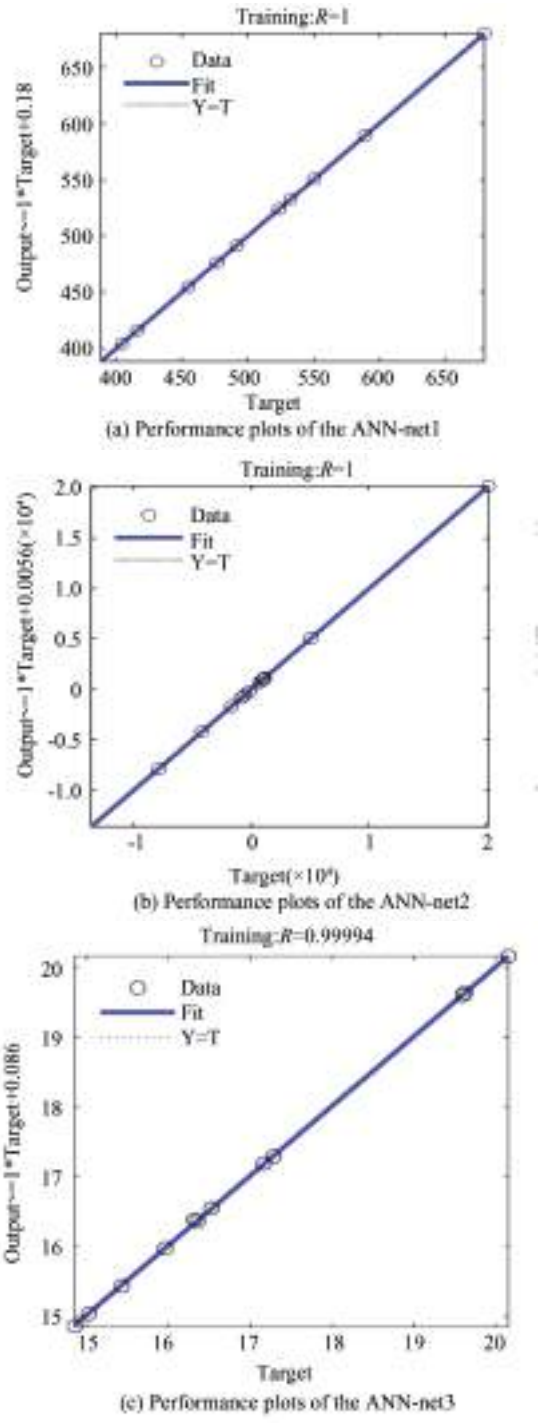

(a) Performance plots of the ANN-net1

(b) Performance plots of the ANN-net2

(c) Performance plots of the ANN-net3

Fig. 5 Performance plots of the ANN-net1, ANN-net2 and ANN-net3

The relationship between the target and the output is shown by the R-value. When $R = 1$, the relationship between the objectives and the outcomes is perfectly linear. There is no linear relationship between targets and outputs when R is close to zero[29]. The predicted data are listed in Table 7.

Table 7 Experimental and predicted result of ANN

No.	Experimental Data			Predicted Output		
	Desired Data			Model Output		
	H. V	RSs	Grain	H. V	RSs	Grain
1	476.387	53	20.157	435.390	41.51	20.155
2	404.467	−173	19.625	407.183	−173.00	19.631
3	550.525	−67	18.024	551.374	−67.00	16.654
4	416.276	110	19.600	530.896	86.25	19.598
5	589.147	−35	20.113	588.683	−49.77	20.003
6	491.510	−113	16.313	489.161	−113.00	16.390
7	454.979	−86	17.285	461.630	−86.00	17.290
8	448.163	−239	16.523	449.178	−238.99	16.549
9	476.387	72	17.167	481.368	72.00	17.192
10	599.437	81	15.275	578.517	81.00	15.678
11	515.580	−57	14.854	515.986	−57.00	14.864
12	532.623	−96	15.960	532.204	−96.00	15.977
13	523.998	42	15.428	530.291	42.00	15.436
14	679.660	53	15.240	674.362	53.00	16.020
15	454.979	68	16.354	510.874	68.00	16.365
16	550.525	85	15.025	550.796	85.99	15.041

4.3 Predicting of Hardness using ANN

The test values for the hardness experiment results are contrasted with the ANN findings displayed in Table 8. The ANN estimation gives the maximal hardness for experiment No. 14, whereas experiment No. 2 gives the lowest one. This demonstrates that the middle hardness levels can be predicted by the ANN more accurately than the lower and higher values. In the upcoming sections, this circumstance will be covered in more detail along with accompanying error graphs. Fig. 6 represents the experimental and ANN results in accordance with all of these. Although the ANN values are generally a little greater than that of the experimental values.

Table 8 Estimation of hardness using ANN

Experiment No.	Concentration Vf (%)	Nanofluids	Temperature C(℃)	Time (min)	Hardness H.V (ANN)
1	0.5	1	850	30	435.39
2	1.0	1	900	30	407.18
3	2.5	1	950	60	551.37
4	5.0	1	1000	60	530.89
5	0.5	2	900	60	588.68
6	1.0	2	850	60	489.16
7	2.5	2	1000	30	461.63
8	5.0	2	950	30	449.17
9	0.5	3	950	30	481.36
10	1.0	3	1000	30	578.51
11	2.5	3	850	60	515.98
12	5.0	3	900	60	532.20
13	0.5	4	1000	60	530.29
14	1.0	4	950	60	674.36
15	2.5	4	900	30	510.87
16	5.0	4	850	30	550.79

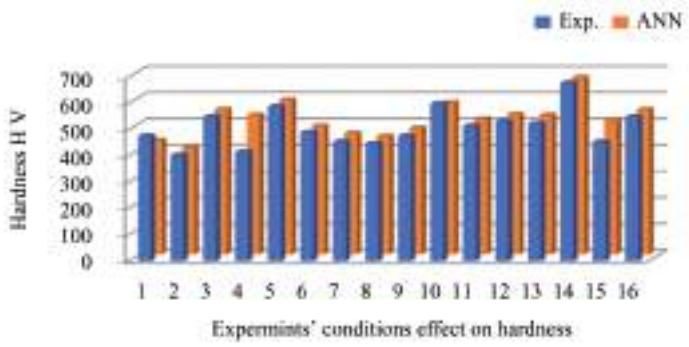

Fig. 6 Comparison of experimental results of hardness with its ANN prediction

4.4 Predicting of Grain Size using ANN

Similar to the prior section, 16 specimen values from Table 6 were used for the ANN analysis of grain size. The ANN estimation outcomes shown in Table 9 were discovered via the trained algorithm, as shown in Fig. 7. The experiment with soaking time of 30 min, and a concentration value of 0.5%, of nanofluid of category one achieved the biggest grain size value, whereas Experiment No. 11, with a concentration value of 2.5%, of nanofluids of category three with soaking time of 60 min, produced the smallest grain size value. These results exhibit the same trend as the experimental findings. In that regard, it is predicted that the error values will be lower than the hardness values. Therefore, it can be asserted that the estimation of grain size would benefit the most from this ANN model.

Table 9 Estimation of grain size using ANN

Experiment No.	Concentration Vf (%)	Nanofluids	Temperature C(℃)	Time (min)	Grain (ANN)
1	0.5	1	850	30	20.155
2	1.0	1	900	30	19.631
3	2.5	1	950	60	16.654
4	5.0	1	1000	60	19.598
5	0.5	2	900	60	20.003
6	1.0	2	850	60	16.390
7	2.5	2	1000	30	17.290
8	5.0	2	950	30	16.549
9	0.5	3	950	30	17.192
10	1.0	3	1000	30	15.678
11	2.5	3	850	60	14.864
12	5.0	3	900	60	15.977
13	0.5	4	1000	60	15.436
14	1.0	4	950	60	16.020
15	2.5	4	900	30	16.365
16	5.0	4	850	30	15.041

4.5 Predicting of Residual Stress Using ANN

Based on the experimental findings in Table 6, the residual stress values were predicted, as shown in Fig. 8. The ANN findings shown in Table 10 were discovered by the trained ANN algorithm. There is a clear parallel between the ANN results and the overall experimental outcomes. However, Experiment No. 4 revealed the maximum tensile residual stress, while Experiment No. 8 presented the minimal compressive residual stress case.

4.6 Errors of Proposed ANN Model

The ANN results presented in the previous sections have different errors, depending on the material mechanical properties. The absolute error is computed using the formula:

$$\text{Error} = |\ \text{real-expected}\ | \tag{3}$$

And the percentage error is calculated using the below formula:

$$\text{Error}\% = \frac{|\text{real-expected}|}{\text{real}} \times 100\% \quad (4)$$

However, the maximal percentage error has been found to be around 1.59%, using the formula:

$$\text{Total error}\ \% = \frac{\sum_{i=1}^{N} E_i}{N} \times 100 \quad (5)$$

where, E_i and N indicate the ANN absolute percentage errors given in Tables 11, 12, and 13. The number of tests for all mechanical tests (i.e., $N = (3 \times 16)$), respectively.

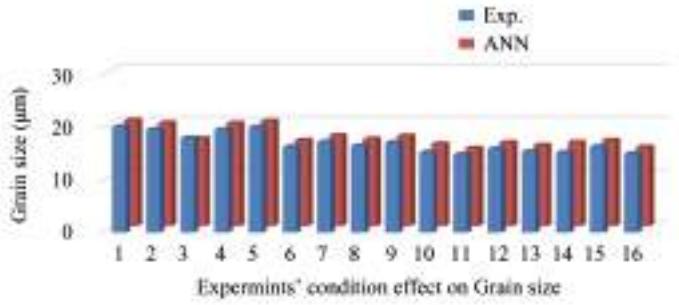

Fig.7 Comparison of the results of grain size with the ANN prediction

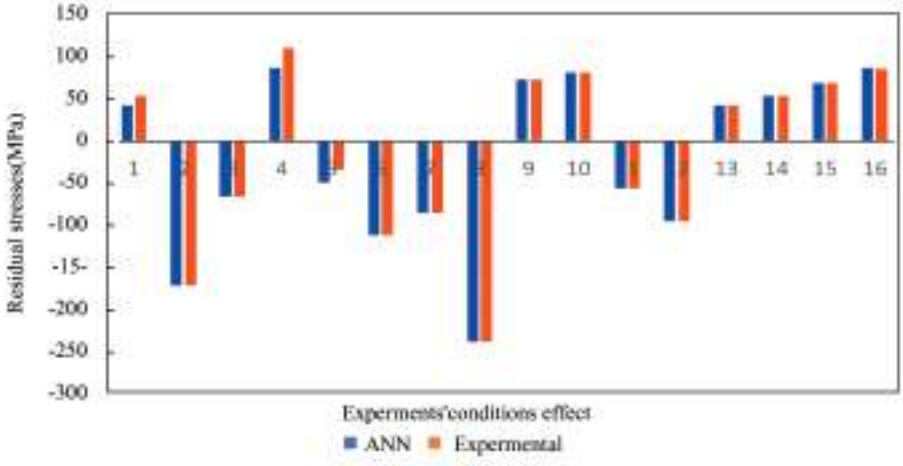

Fig. 8 Comparison results of the residual stress with the ANN predictions

Table 10 Estimation of RSs using ANN

Experiment No.	Concentration Vf(%)	Nanofluids	Temperature C(℃)	Time(min)	RSs (ANN)(MPa)
1	0.5	1	850	30	41.51
2	1.0	1	900	30	−173.00
3	2.5	1	950	60	−67.00
4	5.0	1	1000	60	86.25
5	0.5	2	900	60	−49.77
6	1.0	2	850	60	−113.00
7	2.5	2	1000	30	−86.00
8	5.0	2	950	30	−238.99
9	0.5	3	950	30	72.00
10	1.0	3	1000	30	81.00
11	2.5	3	850	60	−57.00
12	5.0	3	900	60	−96.00
13	0.5	4	1000	60	42.00
14	1.0	4	950	60	53.00
15	2.5	4	900	30	68.00
16	5.0	4	850	30	85.99

Table 11 ANN test errors for hardness

Experiment No.	Concentration Vf (%)	Nanofluid	Temperature C(℃)	Time(min)	Error	Error (%)
1	0.5	1	850	30	40.998	8.606
2	1.0	1	900	30	2.716	0.672
3	2.5	1	950	60	0.849	0.154
4	5.0	1	1000	60	114.620	27.535
5	0.5	2	900	60	0.464	0.079
6	1.0	2	850	60	2.349	0.478
7	2.5	2	1000	30	6.651	1.462
8	5.0	2	950	30	1.015	0.226
9	0.5	3	950	30	4.981	1.046
10	1.0	3	1000	30	20.920	3.490
11	2.5	3	850	60	0.406	0.079
12	5.0	3	900	60	0.418	0.079
13	0.5	4	1000	60	6.294	1.201
14	1.0	4	950	60	5.299	0.780
15	2.5	4	900	30	55.895	12.285
16	5.0	4	850	30	0.271	0.049

Since this study uses four separate experimental mechanical tests, the overall variance percentage is acceptable. As a result, every trial contains experimental errors that could have an impact on the ANN algorithm´s outcomes.

Table 12 ANN test errors for grain size

Experiment No.	Concentration Vf (%)	Nanofluid	Temperature (℃)	Time(min)	Error	Error (%)
1	0.5	1	850	30	0.00	0.01
2	1.0	1	900	30	0.00	0.03
3	2.5	1	950	60	1.37	7.59
4	5.0	1	1000	60	0.00	0.01
5	0.5	2	900	60	0.11	0.54
6	1.0	2	850	60	0.07	0.47
7	2.5	2	1000	30	0.00	0.02
8	5.0	2	950	30	0.02	0.15
9	0.5	3	950	30	0.02	0.14
10	1.0	3	1000	30	0.40	2.63
11	2.5	3	850	60	0.01	0.06
12	5.0	3	900	60	0.01	0.10
13	0.5	4	1000	60	0.00	0.04
14	1.0	4	950	60	0.78	5.11
15	2.5	4	900	30	0.01	0.06
16	5.0	4	850	30	0.01	0.10

Table 13 Results of the ANN test errors for RSs

Experiment No.	Concentration Vf (%)	Nanofluid	Temperature(℃)	Time(min)	Error	Error (%)
1	0.5	1	850	30	11.48	0.21
2	1.0	1	900	30	0	0
3	2.5	1	950	60	0	0
4	5.0	1	1000	60	23.74	0.21
5	0.5	2	900	60	14.77	0.42
6	1.0	2	850	60	0	0
7	2.5	2	1000	30	0	0
8	5.0	2	950	30	0.01	0
9	0.5	3	950	30	0	0
10	1.0	3	1000	30	0	0
11	2.5	3	850	60	0	0
12	5.0	3	900	60	0	0
13	0.5	4	1000	60	0	0
14	1.0	4	950	60	0	0
15	2.5	4	900	30	0	0
16	5.0	4	850	30	0.99	0.01

4.7 Performance Criteria

In order to evaluate the performance of proposed ANN model, R^2, and RMSE criteria are adopted for assessment purposes[27]. The result of experimental and ANN are listed in Table 7 are used in formula (6) to calculate R^2[29,45].

$$R^2 = \frac{\sum_{i=1}^{n} (k_{\exp,i} - K_{\mathrm{EXP}})(k_{\mathrm{ANN},i} - K_{\mathrm{ANN}})}{\sqrt{\sum_{i=1}^{n} ((k_{\exp,i} - K_{\mathrm{EXP}})^2 (k_{\mathrm{ANN},i} - K_{\mathrm{ANN}})^2)}} \quad (6)$$

where $k_{\exp}$, k_{ANN} are represent experimental, and predicted ANN results.

K_{EXP}, K_{ANN} are evaluated by formula (7), and (8):

$$K_{\mathrm{EXP}} = \frac{1}{n} \sum_{i=1}^{n} k_{\mathrm{EXP},i} \quad (7)$$

$$K_{\mathrm{ANN}} = \frac{1}{n} \sum_{i=1}^{n} k_{\mathrm{ANN},i} \quad (8)$$

$$\mathrm{RMSE} = \sqrt{\frac{\sum_{i=1}^{n} (k_{\exp,i} - k_{\mathrm{ANN},i})^2}{n}}$$

The results of Table 7 are used to calculate RMSE value for the result of experimental and expected result of ANN model. The minimum value of RMSE is achieved by the predicted result of grain size which is 0.025.

5 Conclusions

The effects of heat treatment on the mechanical properties of AISI 1035 were examined in this study. To enhance the mechanical properties of a medium carbon steel alloy, various quenching mediums of nanofluid are proposed. Also, suggested is a model for predicting the mechanical properties of AISI 1035 during the quenching process using an artificial neural network (ANN). The following conclusions can be drawn from the obtained results:

1) Quenching AISI 1035 using nanofluids is promising but requires the careful adjustment of the volume concentration of the nanoparticles.

2) The highest compressive residual stress of 239 MPa was attained under the following conditions: oil/CuO, a CuO volume fraction of 5%, a temperature of 950 ℃, and a soaking period of 30 min.

3) The maximum hardness was 679.6 HV, which was achieved at conditions of water/hybrid nanoparticles 75% CuO + 25% TiO_2, temperature 950 ℃, and a 60 min soaking time.

4) The refinement of grain size was 14.854 μm, which was achieved at a concentration ratio of nanoparticles of 2.5 vf %, engine oil/Al_2O_3, a temperature 850 ℃, and 60 min soaking time.

5) The outcomes showed that all conditions led to a noticeable improvement in the alloy's hardness which reached 100%, the grain size is refined about 80%, and unwanted residual stresses is removed from 50 to 150 MPa

6) Statistical analysis of MANOVA showed that the nanofluid type had significant effect on the responses of hardness, grain size, and residual stresses. P values are 0.029, and 0.01 for Wilks', and Lawley-Hotelling criteria respectively.

7) Performance of ANN model is evaluated based on R^2 value which approached to 1. The value indicates a good performance for the proposed model.

8) For the parameters of residual stresses, hardness, and particle size, the provided ANN model fits well with the experimental findings.

9) The proposed ANN model has a better agreement with the expected results of residual stresses and hardness values than it does with the projected outcome of grain size.

10) Percentage error, R^2, and RMSE indicate an acceptable impression for proposed ANN model.

Acknowledgment

The authors would like to thankful Kut Technical Institute for their funding supports.

References

[1] Hussein A K, Abbas Laith K, Hasan Wisam N. Effect of quenching media variations on the mechanical behavior of martensitic stainless steel. Al-Khwarizmi Engineering Journal, 2019, 15(2): 1-12. DOI: 10.22153/kej.2019.11.002.

[2] Samuel A, Prabhu K N. Residual stress and distortion during quench hardening of steels: a review. Journal of Materials Engineering and Performance, 2022, 31(7): 5161-5188.

[3] Aldriasawi Salman Khayoon, Nihayat Hussein Ameen, Kamyapithode, et al. Electromagnetic properties, forming limit diagrams and fracture toughness of laminated Al/Fe_2O_3 composites.Surface Review and Letters, 2023,DOI: 10. 1142/S0218625X24500227. https://www. worldscientific. com/doi/10.1142/S0218625X24500227.

[4] Babu K, Arularasan R, Srinath Ramkumar S. Quenching performance of AISI 1010 in CNT nanofluids. Materials Today: Proceedings, 2017,4(10): 11044-11049.DOI: 10.1016/j.matpr.2017.08.065

[5] Abbas Hussein, Laith K Abbas, Wisam Hasan. Optimization of heat treatment parameters for the tensile properties of medium carbon steel. Engineering and Technology Journal, 2018,36(10A): 1091-1099.DOI: 10.30684/etj.36.10A.10.

[6] Mohammad Hemmat Esfe, Fatemeh Zabihi, Hossein Rostamian, et al. Experimental investigation and model development of the non-Newtonian behavior of CuO-MWCNT-10w40 hybrid nano - lubricant for lubrication purposes. Journal of Molecular Liquids, 2018, 249: 677-687.DOI:10.1016/j.molliq.2017.11.020.

[7] Kresnodrianto Harjanto S, Putra W N, Ramahdita G, et al. Characterization of water based nanofluid for quench medium. IOP Conference Series: Materials Science and Engineering. Bristol: IOP Publishing, 2018, 348(1): 012009.DOI:10.1088/1757-899X/348/1/012009.

[8] Sakeena Yahya, Sri Harjanto, Wahyuaji Narottama Putra, et al. Characterization and observation of water-based nanofluids quench medium with carbon particle content variation. Proceedings of the International Seminar on Metallurgy and Materials: Metallurgy and Advanced Material Technology fo rSustainable Development. AIP Publishing, 2018, 1964(1): 020006. DOI: 10. 1063/1.5038288.

[9] Dhinesh Kumar Devendiran, Valan Arasu Amirtham. A review on preparation, characterization, properties and applications of nanofluids. Renewable and Sustainable Energy Reviews, 2016, 60: 21-40. DOI: 10.1016/j.rser.2016.01.055.

[10] Salman K D, Khalifa M Z. Improving the mechanical properties of CK35 steel using ND: yag laser surface hardening. Journal of Engineering and Sustainable Development, 2016, 20(2): 250-258.

[11] Lee J-M, Han J-J, Song Y-B,et al., Microstructure and mechanical properties of the high-hardness armor steels. Korean Journal of Materials Research,2018,28(8):459-465.DOI:10.3740/MRSK.2018.28.8.459.

[12] Salman K, Ahmed B A, Frhan I N. Effect of quenching media on mechanical properties of medium carbon steel 1030. Journal of University of Babylon for Engineering Sciences, 2018,26(2): 214-222.

[13] Simencio Otero R L, Canale Lauralice C F, Totten G E, et al. Vegetable oils as metal quenchants: a comprehensive review.Materials Performance and Characterization, 2017, 6(1): 174-250.DOI:10.1520/MPC20160112.

[14] da Silva A D, Pedrosa T A, Gonzale-Mendez J L, et al. Distortion in quenching an AISI 4140 C-ring-Predictions and experiments. Materials & Design, 2012, 42: 55-61. DOI;10.1016/j.matdes.2012.05.031.

[15] Powar A, Date P. Modeling of microstructure and mechanical properties of heat treated components by using Artificial Neural Network. Materials Science and Engineering: A, 2015, 628: 89-97. DOI: 10. 1016/j.msea.2015.01.044.

[16] Yang X-W, Zhu J-C, Nong Z-S, et al. Prediction of mechanical properties of A357 alloy using artificial neural network. Transactions of Nonferrous Metals Society of China, 2013, 23(3): 788-795. DOI: 10. 1016/S1003-6326(13)62530-3.

[17] Mahalle G, Salunke O, Kotkunde N, et al. Neural network modeling for anisotropic mechanical properties and work hardening behavior of Inconel 718 alloy at elevated temperatures. Journal of Materials Research and technology, 2019, 8(2): 2130-2140. DOI: 10.1016/j.jmrt.2019.01.019.

[18] Wang Y, Sha A, Li X, et al. Prediction of the mechanical properties of titanium alloy castings based on a back-propagation neural network. Journal of Materials Engineering and Performance, 2021, 30: 8040-8047.

[19] Maleki E, Unal O. Shot peening process effects on metallurgical and mechanical properties of 316 L steel via: experimental and neural network modeling. Metals and Materials International, 2021, 27: 262-276.

[20] Maleki E, Unal O. Fatigue limit prediction and analysis of nano-structured AISI 304 steel by severe shot peening via ANN. Engineering with Computers, 2021, 37(4): 2663-2678.

[21] Maleki E, Unal O. Optimization of shot peening effective parameters on surface hardness improvement. Metals and Materials International, 2021, 27: 3173-3185.

[22] Kara F, Özbek O, Özbek N A, et al. Investigation of the effect of deep cryogenic process on residual stress and residual austenite. Gazi Mühendislik Bilimleri Dergisi, 2021, 7(2): 143-151. DOI: 10.30855/gmbd.2021.02.07.

[23] Nas E, Özbek O, Bayraktar F, et al. Experimental and statistical investigation of machinability of AISI D2 steel using electroerosion machining method in different machining parameters. Advances in Materials Science and Engineering, 2021, 2021: Article ID 1241797. DOI: 10.1155/2021/1241797.

[24] Salman K H, Elsheikh Ammar H, Ashham M, et al. Effect of cutting parameters on surface residual stresses in dry turning of AISI 1035 alloy. Journal of the Brazilian Society of Mechanical Sciences and Engineering, 2019, 41(8): 1-12.

[25] Alawi Omer A, Che Sidik N A, Xian H W, et al. Thermal conductivity and viscosity models of metallic oxides nanofluids. International Journal of Heat and Mass Transfer, 2018, 116: 1314 - 1325. DOI: 10.1016/j.ijheatmasstransfer.2017.09.133.

[26] Davis R, John P. Application of Taguchi-based design of experiments for industrial chemical processes. Statistical approaches with emphasis on design of experiments applied to chemical processes. 2018: 137. DOI: 10.5772/intechopen.69501

[27] Kara F, Bayraktar F, Savas F, et al. Experimental and statistical investigation of the effect of coating type on surface roughness, cutting temperature, vibration and noise in turning of mold steel. Journal of Materials and Manufacturing, 2023, 2(1): 31 - 43. DOI: 10.5281/zenodo.8020553.

[28] Syam Sundar L, Sharma K V, Singh Manoj K, et al. Hybrid nanofluids preparation, thermal properties, heat transfer and friction factor-a review. Renewable and Sustainable Energy Reviews, 2017, 68: 185-198. DOI: 10.1016/j.rser.2016.09.108.

[29] Maleki E, Unal O, Kashyzadeh K R. Fatigue behavior prediction and analysis of shot peened mild carbon steels. International Journal of Fatigue, 2018, 116: 48-67. DOI: 10.1016/j.ijfatigue.2018.06.004.

[30] Taha O M E, Majeed Z H, Ahmed S M. Artificial neural network prediction models for maximum dry density and optimum moisture content of stabilized soils. Transportation Infrastructure Geotechnology, 2018, 5: 146-168.

[31] Aburas M M, Ahamad Mohd Sanusi S, Omar N Q. Spatio-temporal simulation and prediction of land-use change using conventional and machine learning models: A review. Environmental Monitoring and Assessment, 2019, 191: 1-28.

[32] Jahanshahi M, Maleki E, Ghiami A. On the efficiency of artificial neural networks for plastic analysis of planar frames in comparison with genetic algorithms and ant colony systems. Neural Computing and Applications, 2017, 28: 3209-3227.

[33] Zhao J, Ding H, Zhao W, et al. Modelling of the hot deformation behaviour of a titanium alloy using constitutive equations and artificial neural network. Computational Materials Science, 2014, 92: 47-56. DOI: 10.1016/j.commatsci.2014.05.040.

[34] Maleki E, Unal O, Kashyzadeh K R. Surface layer nanocrystallization of carbon steels subjected to severe shot peening: Analysis and optimization. Materials Characterization, 2019, 157: 109877. DOI; 10.1016/j.matchar.2019.109877.

[35] Erkan Ö, I ık B, Çiçek A, et al. Prediction of damage factor in end milling of glass fibre reinforced plastic composites using artificial neural network. Applied Composite Materials, 2013, 20: 517-536.

[36] Maleki E, Unal O, Sahebari S M S, et al. Application of deep neural network to predict the high-cycle fatigue life of AISI 1045 steel coated by industrial coatings. Journal of Marine Science and Engineering, 2022, 10(2): 128. DOI: 10.3390/jmse10020128.

[37] Merayo D, Rodríguez-Prieto A, Camacho A M. Prediction of mechanical properties by artificial neural networks to characterize the plastic behavior of aluminum alloys. Materials, 2020, 13 (22): 5227. DOI: 10.3390/ma13225227.

[38] Kong D, Dong C, Ni X, et al. Mechanical properties and corrosion behavior of selective laser melted 316L stainless steel after different heat treatment processes. Journal of Materials Science & Technology, 2019, 35(7): 1499-1507. DOI: 10.1016/j.jmst.2019.03.003.

[39] Wu J, Wei P, Liu H, et al. Evaluation of pre-shot peening on improvement of carburizing heat treatment of AISI 9310 gear steel. Journal of Materials Research and Technology, 2022, 18: 2784-2796. DOI: 10.1016/j.jmrt.2022.03.163.

[40] Li M, Chen W-Y, Zhang X. Effect of heat treatment on creep behavior of 316 L stainless steel manufactured by laser powder bed fusion. Journal of Nuclear Materials, 2022, 559: 153469.DOI:10.1016/j.jnucmat.2021.153469.

[41] Wang X, Shi X, Hui Y, et al. Mechanical behavior and strengthening mechanism of a fine-grained medium carbon steel produced via cyclic oil quenching. Materials Science and Engineering: A, 2023, 866: 144669. DOI:10.1016/j.msea.2023.144669.

[42] Balavar M, Mirzadeh H. Enhancement of mechanical properties of low carbon steel based on heat treatment and thermo-mechanical processing routes. Journal of Ultrafine Grained and Nanostructured Materials, 2018, 51(2): 169-173.DOI:10.22059/jufgnsm.2018.02.09.

[43] Meng L, Li W, Shi Q, et al. Effect of partitioning treatment on the microstructure and properties of low-carbon ferritic stainless steel treated by a quenching and partitioning process. Materials Science and Engineering: A, 2022, 851: 143658.DOI:10.1016/j.msea.2022.143658.

[44] Lopez-Garcia R D, Medina-Juárez I, Maldonado-Reyes A. Effect of quenching parameters on distortion phenomena in AISI 4340 steel. Metals, 2022, 12(5): 759. DOI:10.3390/met12050759.

[45] Maleki E, Unal O, Guagliano M, et al. Analysing the fatigue behaviour and residual stress relaxation of gradient nano-structured 316L steel subjected to the shot peening via deep learning approach. Metals and Materials International, 2022, 28: 112-131.DOI:10.1007/s12540-021-00995-8.